

# Tunneling Energy Effects on GC Oxidation in DNA

Glenna S. M. Tong, Igor V. Kurnikov,<sup>†</sup> and David N. Beratan\*

Departments of Chemistry and Biochemistry, Box 90346, Duke University, Durham, North Carolina 27708-0346

Received: September 5, 2001; In Final Form: December 11, 2001

Hole-mediated electronic couplings, reorganization energies, and electron transfer (ET) rates are examined theoretically for hole-transfer reactions in DNA. Electron transfer rates are found to depend critically on the energy gap between the donor/acceptor states and the intervening bases—the tunneling energy gap. The calculated distance decay exponent for the square of the electronic coupling,  $\beta$ , for hole transfer between GC base pairs (and pi-electron D/A pairs) ranges from 0.95 to 1.5 Å<sup>-1</sup> in the model structures as the tunneling energy gap varies from 0.3 to 0.8 eV (which we argue is the range of energy gaps for GC oxidation probed in recent experiments). We show that the tunneling energy gap depends on the ET reorganization energy, which itself grows rapidly with distance for ET over 1–5 base pairs. Inclusion of the distance dependence of reorganization energies for these hole transfer reactions gives the tunneling rates an apparent decay exponent of  $\sim 1.5$ – $2.5$  Å<sup>-1</sup>. We show that ET rates observed in DNA across one and two base pairs are reasonably well described with single-step ET theories, using our calculated couplings and reorganization energies. However, the computed single-step tunneling (superexchange) ET rates for donor and acceptor species separated by three or more base pairs are much smaller than observed. We conclude that longer-distance ET probably proceeds through thermal population of intermediate hole states of the bridging bases. Switching between mechanisms as distance grows beyond a few base pairs is likely to be a general characteristic of ET in small tunneling energy gap systems.

## I. Introduction

In the past decade, long-distance DNA electron transfer (ET) has received considerable experimental<sup>1–43</sup> and theoretical attention.<sup>44–67</sup> A fundamental understanding of these reactions has substantial implications for establishing the mechanism of DNA damage and repair,<sup>68–71</sup> as well as for designing DNA biological assays<sup>72–75</sup> and miniaturized electronic devices.<sup>52,76–85</sup> Our goal is to establish a quantitative physical framework for describing these reactions, based on a detailed molecular-modeling approach. Our specific focus is the nature of superexchange-mediated coupling among native bases, modified bases, and  $\pi$ -electron reaction partners such as stilbene. ET in systems of this kind is probed in a large number of recent experiments<sup>11,12,14,15,17–19,21,23,27,31–35,37–43</sup> involving hole transfer to GC base pairs imbedded in AT runs. We will show that the strong electron–nuclear coupling characteristic of DNA ET leads to tunneling energy gaps of  $\sim 0.5$ – $1.0$  eV between bridging and donor–acceptor states and, consequently, rapid decay of superexchange interactions with ET distance. Therefore, we expect (in this class of DNA ET experiments) a switching of the ET mechanism from superexchange to thermally activated hopping for donor–acceptor pairs separated by more than two base pairs.

**Tunneling versus Hopping.** DNA mediated ET reactions display a wide range of distance dependencies, associated with apparent exponential decay constants from 0.1 to 1.5 Å<sup>-1</sup> (the values at the extremes of this range remain somewhat uncertain as the primary kinetic processes are not easily

probed).<sup>1,9,12,14,15,17–19,24,26,27,31,36,40,41</sup> A physical explanation of this wide range of observed distance dependences is that DNA ET can access either single step donor-to-acceptor tunneling (superexchange) or multistep hopping along the DNA bases.<sup>45–48,51,57,59,65,86,87</sup> If the donor and acceptor interact weakly, the electron-tunneling rate is often described by a nonadiabatic golden rule rate expression (in the high-temperature regime):<sup>88</sup>

$$k_{\text{ET}}^{\text{non-ad}} = \frac{2\pi}{\hbar} |H_{\text{DA}}|^2 \frac{1}{\sqrt{4\pi\lambda k_{\text{B}}T}} \exp\left[-\frac{(\Delta G^0 + \lambda)^2}{4\lambda k_{\text{B}}T}\right] \quad (1)$$

Here,  $H_{\text{DA}}$  is the donor–acceptor interaction mediated by the bridging medium. The  $H_{\text{DA}}$  superexchange interactions decay approximately exponentially with distance and lead to a rapid decay of tunneling ET rates with distance. Exponential decay constants for  $H_{\text{DA}}$  in proteins are  $\sim 1.0$ – $1.5$  Å<sup>-1</sup>,<sup>89–91</sup> and electron tunneling rates drop by about an order of magnitude each 1.0–3.0 Å.<sup>91</sup> Multistep hopping in DNA is possible if donor and/or acceptor groups can oxidize or reduce some of the bases. Rapid multistep hopping can proceed over much larger distance than single-step tunneling.<sup>57,59</sup>

It is important to understand precisely how far and how fast an electron or hole may tunnel in DNA and what factors influence this tunneling process, to understand both single and multistep transport mechanisms. Even in multistep ET, the short distance steps may involve tunneling (if the reaction is nonadiabatic). This paper focuses on the specific structural and energetic aspects of DNA that influence the electron tunneling rates.

DNA hole transfer systems under study in several labs employ donors and acceptors with redox potentials close to those of

\* Corresponding author.

<sup>†</sup> Current address: Department of Chemistry, Northwestern University, Evanston, IL 60208.

the native bases. As such, the tunneling energy gap (the energy difference between the donor, acceptor, and bridge-localized electronic states) is small (tenths of electronvolts).<sup>35b</sup> Since ET occurs in nonequilibrium structures where the donor and acceptor are quasidegenerate, the tunneling energy gap should be computed for these nonequilibrium structures. The key argument made in this paper is that this relatively small tunneling energy gap makes the DNA hole-transfer mechanism qualitatively different from that in most protein ET processes. The smaller tunneling energy gap in DNA causes ET to be particularly sensitive to details of the donor and acceptor energetics and solvation, and to DNA geometry. We explore the nature of hole tunneling and transport in this small tunneling energy gap regime, making specific contact with recent experiments from Lewis' lab<sup>31</sup> involving GC oxidation.

The structure of this paper is as follows: section II describes the rate theory for DNA ET, emphasizing the role of the tunneling energy gap; section III describes the computational methods; section IV applies the analysis in detail to  $^{+}\text{GC}/(\text{AT})_n/\text{GC}$  ET; section V examines the experimental systems of Lewis and co-workers— $\text{St}^*/(\text{AT})_n/\text{GC}$  ( $\text{St}$  = stilbene).<sup>31</sup> Section VI summarizes our conclusions. The appendices describe (1) the determination of the tunneling energies in a linear-response approximation, (2) the methods used to compute the tunneling interactions, (3) the reorganization energy computations, and (4) the  $\text{St}$ –GC couplings calculations.

## II. Defining the Tunneling Energy for DNA Hole Transfer

In B-DNA, the electronic interactions between neighboring base pairs are approximately 0.1–0.2 eV.<sup>61,62</sup> The interactions between second neighbors are several times weaker (vide infra). As such, ET between second-neighbor (or more distant) base pairs is expected to fall well within the nonadiabatic regime.<sup>88</sup>

The DNA ET reactions discussed in this paper involve the oxidation of guanine bases. These studies complement other DNA ET experiments that involve appended donors and acceptors.<sup>1–8,24,25,36,44–46</sup> The donor and acceptor states, including the guanines, have ET active states close in energy (tenths of electronvolts) to the bridging (AT) states. The strength of bridge-mediated coupling is expected to vary strongly with the tunneling energy gap (the energy gap between the donor/acceptor states and the intervening bases) in this regime of near resonance. As such, it is critical to examine this gap in greater detail. We show that vibronic interactions associated with formation of the activated complex play an important role in determining this gap.

One can identify inner- and outer-sphere vibronic interactions that influence donor, acceptor, and bridge state energetics in DNA. Inner-sphere contributions are associated with changes of the redox-center geometries on reduction or oxidation. Outer-sphere contributions are determined by changes in solvation coupled to the ET reaction. All of these vibronic interactions cause a stabilization of the charged states (compared to frozen geometries) and lead to broadening of the energy levels as well. The vibronic coupling effects are visualized in the donor and acceptor spectral function picture.<sup>93</sup> The spectral functions represent the probability of inserting (on the acceptor) or removing (from the donor) electrons with a given energy. In the high-temperature linear-response approximation, these spectral functions are Gaussians with variance  $\sigma^2 = \lambda kT$  (see Appendix 1). Appendix 1 shows that the offset between spectral function peaks at zero reaction free energy is equal to the ET reorganization energy  $\lambda$  (recall that the rate is a maximum when

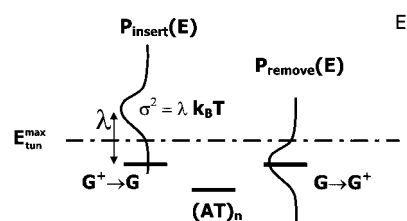


**Figure 1.** Spectral functions  $[P(E)]$  for electron insertion and removal for  $\text{G}^{+}$  to  $\text{G}$  hole transfer. The vertical axis ( $E$ ) represents the energy for electron removal (from the donor) and insertion (on the acceptor). The  $P(E)$  curves represent the probability of inserting or removing an electron with a particular energy. The  $-\text{IP}$  of guanine in a vacuum is indicated by the thick horizontal bars in the figure. The most probable value of the tunneling energy ( $E_{\text{tun}}^{\text{max}}$ ) is shifted from the guanine vacuum  $-\text{IP}$  value by  $\lambda/2$ . The  $-\text{IP}$  associated with the bridging  $(\text{AT})_n$  states is also indicated. The variance of the insertion and removal functions is  $\sigma^2$  (the relation between  $\sigma^2$  and the reorganization energy  $\lambda$  is discussed in Appendix 1).

$-\Delta G^{\circ} = \lambda$ ). For neutral donors (acceptors), these functions are peaked approximately around a (minus) “gas-phase” vertical ionization potential (electron affinity). Figure 1 shows a qualitative view of the insertion and removal spectral functions associated with hole transfer from  $\text{GC}^{+}$  to  $\text{GC}$ . The energy offset between the two peaks appears because the guanine radical cation is solvated, and its equilibrium geometry is different from that of neutral guanine. The overlap of the spectral functions gives the rate of nonadiabatic electron transfer via

$$k_{\text{ET}}^{\text{non-ad}} = \frac{2\pi}{\hbar} \int_{-\infty}^{\infty} |H_{\text{DA}}(E_t)|^2 P_{\text{insert}}(E_t) P_{\text{remove}}(E_t) dE_t \quad (2)$$

$E_t$  in eq 2 is the electron tunneling energy. The ET process is most likely to occur at a tunneling energy where the product of the donor ( $P_{\text{remove}}(E_t)$ ) and acceptor ( $P_{\text{insert}}(E_t)$ ) spectral functions is peaked,  $E_t^{\text{max}}$ . If  $P_{\text{insert}}(E_t)$  and  $P_{\text{remove}}(E_t)$  have equal widths, their product reaches a maximum at the average of the two peak positions,  $E_t^{\text{max}}$ . If  $H_{\text{DA}}$  depends weakly on the tunneling energy or the product of the spectral functions is sufficiently narrow, eq 2 can be simplified.  $H_{\text{DA}}$  can be factored outside of the integral in eq 2 and evaluated at the tunneling energy  $E_t^{\text{max}}$ :

$$k_{\text{ET}}^{\text{non-ad}} \approx \frac{2\pi}{\hbar} |H_{\text{DA}}(E_t^{\text{max}})|^2 \int_{-\infty}^{\infty} P_{\text{insert}}(E_t) P_{\text{remove}}(E_t) dE_t \quad (3)$$

Equation 3 is one form of the Condon approximation for ET reactions (a second type of Condon approximation is associated with using a single DNA conformation as defined by a set of torsion angles). When the tunneling energy gap is sufficiently small, however,  $H_{\text{DA}}(E_t)$  has a strong dependence on the tunneling energy (see section IV). In the case of very small tunneling energy gaps, evaluating  $H_{\text{DA}}$  at a single tunneling energy and factoring it outside of the integral in eq 2 can be a poor approximation.<sup>93b</sup>

An important consequence of the tunneling energy considerations (above and in Appendix 1) is that the most probable tunneling energy  $E_t^{\text{max}}$  lies above the (negative) vertical vacuum ionization potential of the donor (see Figure 1). This offset shifts the tunneling energy away from the occupied bridge eigenstates, weakening the donor–acceptor interactions and increasing the distance decay constant,  $\beta$ .

Below, we show that estimated tunneling energy offsets (equal to  $\lambda/2$ ) from gas-phase orbital energies for DNA ET are between 0.25 and 0.8 eV, on the same order or larger than the tunneling energy gaps estimated from “gas-phase” quantum chemical computations of the relative IPs of DNA bases. As such,

consideration of solvent and inner-sphere reorganization energies are essential to make meaningful estimates of the tunneling energy gaps and donor/acceptor couplings in DNA ET reactions.

### III. Methods to Calculate ET Reaction Parameters

Several simulation techniques are used here to calculate donor–acceptor interactions and ET reorganization energies. Some of these methods are well established, while others require testing for the DNA ET problem. One goal of this paper is to advance the methodology for quantitative and predictive calculations of DNA ET parameters.

**Electronic Coupling.** Appendix 2 describes methods we used to calculate donor–acceptor electronic couplings. Perhaps the most widely used method to compute  $H_{DA}$  values is the computation of the “minimum energy splitting” between the donor and acceptor localized orbitals.<sup>94–97</sup> This methodology, and our implementation, is described in Appendix 2A.

Splitting calculations require multiple Hamiltonian matrix diagonalization. We have developed an approach that uses the Green’s function matrix elements involving the donor and acceptor states.<sup>98</sup> The Green’s function matrix elements are computed from a single matrix inversion. Similar strategies can be used to compute electronic couplings for more involved electronic structure methods. This methodology is described in Appendix 2B. A third approach to computing electronic coupling interactions involves perturbation theory. This method, also described in Appendix 2B, allows tunneling energy analysis of the electronic coupling.

Finally, we explored the applicability of a divide-and-conquer (D&C) approach for building the DNA electronic Hamiltonian based on fragment calculations. This approach is useful when conventional Hartree–Fock analysis is beyond reach because of system size. This method is described in Appendix 2C.

**Reorganization Energy.** Appendix 3 describes the outer-sphere reorganization energy calculations. These methods were employed previously to analyze ET reactions.<sup>99–101</sup> Similar methods were used recently by Fayer to study DNA reorganization energies.<sup>102</sup>

### IV. Model DNA ET Systems: Electronic Coupling across AT Stacks to Guanine (G) or 7-Deaza-Guanine (Z).

We first examine model ET systems consisting of AT stacks between donors and acceptors. The donor/acceptor pairs that we analyze are guanine/guanine radical cation ( $G/G^{\bullet+}$ ) and 7-deaza-guanine/7-deaza-guanine radical cation ( $Z/Z^{\bullet+}$ ). Z is easier to oxidize than G by a few tenths of 1 eV. Systems of this kind were studied recently in the groups of Giese,<sup>17–19,21,23,103</sup> Barton,<sup>9–13,104</sup> Lewis,<sup>27,31–35</sup> and Fukui.<sup>14–16</sup> The  $ZC/(AT)_n/ZC$  and  $GC/(AT)_n/GC$  ( $n = 1–4$ ) systems used in our analysis were taken in the standard B-form. Most coupling calculations were performed on structures with the sugar–phosphate backbone removed (H-atom capping was used in these structures). Coupling calculations were based on Hartree–Fock analysis using a 3-21G basis set, as discussed in the Appendix 2. The influence of the backbone and basis set on the couplings is analyzed below.

**Distance Dependence of  $H_{DA}$ .** The distance dependences of  $H_{DA}$  in  $ZC/(AT)_n/ZC$  and  $GC/(AT)_n/GC$  (no backbone included) are shown in Figure 2. The coupling matrix elements decay approximately exponentially with distance:

$$H_{DA}(R) = H_{DA}^0 \exp\left[-\frac{\beta}{2}(R - R_{DA})\right] \quad (4)$$

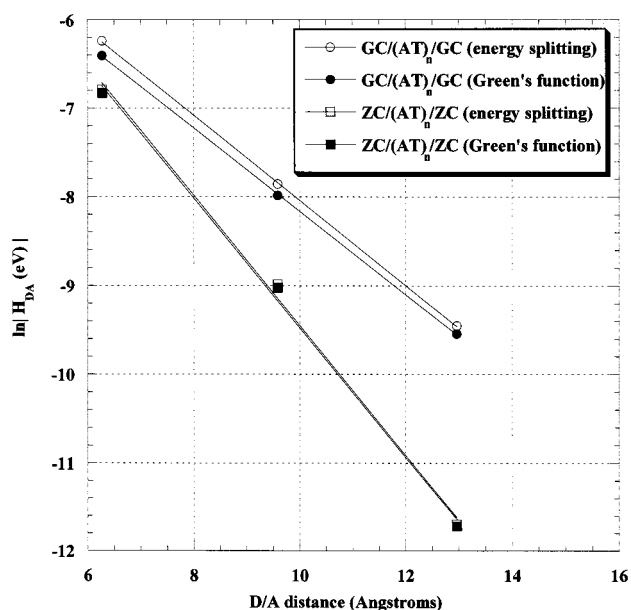


Figure 2. Distance dependence of computed  $H_{DA}$  in  $GC/(AT)_n/GC$  and  $ZC/(AT)_n/ZC$ .

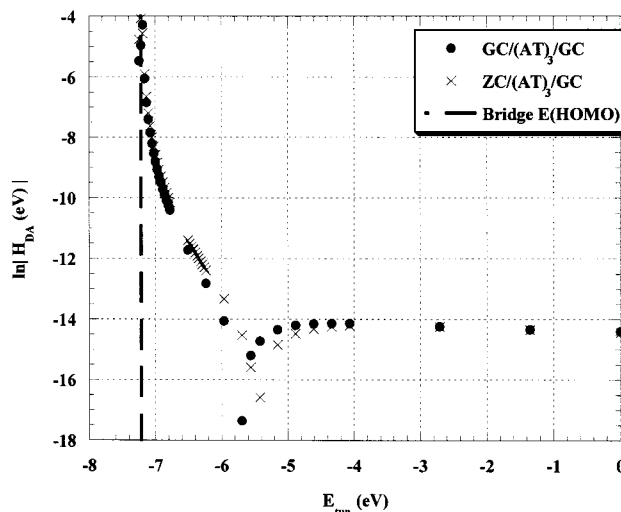
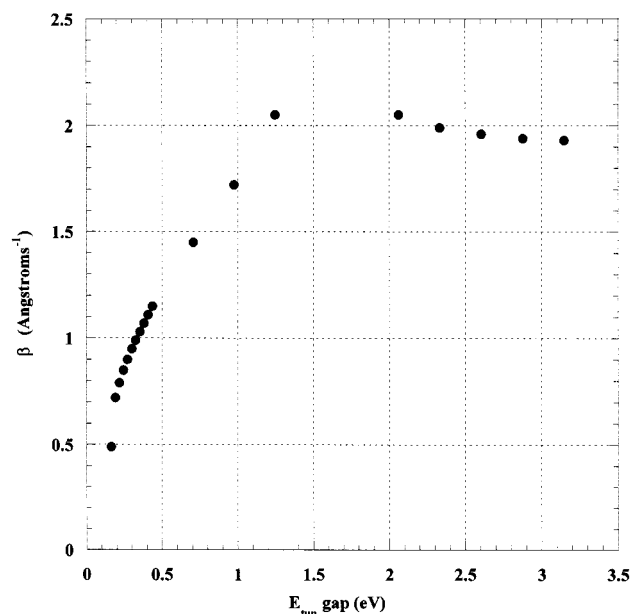


Figure 3. Tunneling energy dependence of  $H_{DA}$  for  $GC/(AT)_3/GC$  and  $ZC/(AT)_3/ZC$ .

$H_{DA}$  values for both GC and ZC systems were computed with the minimum energy splitting method and the Green’s function approaches of Appendix 2. The two methods are in excellent agreement, indicating the viability of the faster Green’s function strategy.

The  $\beta$  values were computed to be 0.95 and 1.46  $\text{\AA}^{-1}$  for  $GC/(AT)_n/GC$  and  $ZC/(AT)_n/ZC$ , respectively. As the geometries of the GC and ZC structures are nearly identical, the difference in the distance dependence is attributed to a tunneling energy effect. ZC systems have substantially larger tunneling energy gaps compared to the GC systems. The tunneling energy gap (specifically, the energy gap between the bridge HOMO and the donor/acceptor localized states) is  $\sim 0.7–0.8$  eV for  $ZC/(AT)_n/ZC$  and  $\sim 0.2–0.3$  eV for  $GC/(AT)_n/GC$ . Figure 3 shows the tunneling energy dependence of  $H_{DA}$  for the  $GC/(AT)_3/GC$  and  $ZC/(AT)_3/ZC$  systems computed using the perturbation approach (Appendix 2). This perturbation analysis performed at the energies of the G- and Z-localized orbitals reproduces the values of  $H_{DA}$  obtained using the minimum energy splitting method. Figure 3 shows that the tunneling energy dependences



**Figure 4.** Tunneling energy dependence of  $\beta$  in GC/(AT) $_n$ /GC ( $n = 1-3$ ) systems, assuming that the bridge HOMO energy is  $-7.21$  eV.

of  $H_{DA}$  for GC/(AT) $_3$ /GC and ZC/(AT) $_3$ /ZC are nearly coincident. This indicates that the difference in the coupling values for GC/(AT) $_n$ /GC and ZC/(AT) $_n$ /ZC arises from difference in the tunneling energies.

**Tunneling Energy Dependence of  $\beta$ .** The success of the perturbation formula in reproducing the electronic couplings for GC/(AT) $_n$ /GC and ZC/(AT) $_n$ /ZC allows us to predict superexchange couplings through AT stacks with donors and acceptors that have similar  $\pi$ -electronic structures but different energetics. Figure 4 shows  $\beta$  versus the tunneling energy gap computed in the perturbative analysis based on the Hamiltonians computed for GC/(AT) $_n$ /GC structures. We have assumed that the bridge HOMO energy is  $-7.21$  eV. The distance decay depends only weakly on the tunneling energy when the tunneling energy gap is larger than 2 eV. This plateau  $\beta$  value is about  $2 \text{ \AA}^{-1}$ , even larger than the typical plateau distance decay parameter in proteins of  $1.0-1.5 \text{ \AA}^{-1}$  (depending on the protein structure). However, as the tunneling energy closely approaches the bridge HOMO energy,  $\beta$  decreases rapidly.  $\beta$  is about  $0.5 \text{ \AA}^{-1}$  when the tunneling energy gap is about 0.15 eV. The steep dependence of  $\beta$  on tunneling energy gap in the near-resonant regime is similar to that reported in ref 53 by Siebbeles and co-workers. Siebbeles studied the dependence of  $\beta$  on injection energy ( $<0.7$  eV), which is closely related to the tunneling energy gap. We emphasize that the tunneling energy gap is an energy difference between electronic states in specific activated state geometries and is a fluctuating quantity with a most probable value associated with both the electronic and reorganization energies. We prefer to use the term “injection energy” in reference to the free energy difference between the reduced donor and bridge states. The injection free energy is a thermodynamic quantity, strongly related but not identical to the tunneling energy gap.<sup>35b</sup>

**Reorganization Energy Dependence of the Tunneling Energy.** The distance dependence of  $H_{DA}$  in DNA weakens ( $\beta$  decreases) at smaller tunneling-energy gaps, although  $\beta$  is less than  $1.0 \text{ \AA}^{-1}$  only for tunneling energy gaps below 0.3 eV. We discussed (section II) the fact that vibronic coupling increases the average tunneling energy gap by about  $\lambda/2$ , compared to the gas-phase fixed-geometry analysis. The inner-sphere reorganization energy ( $\lambda_i$ ) for  $G^{+*}$  to  $G$  hole transfer can be estimated

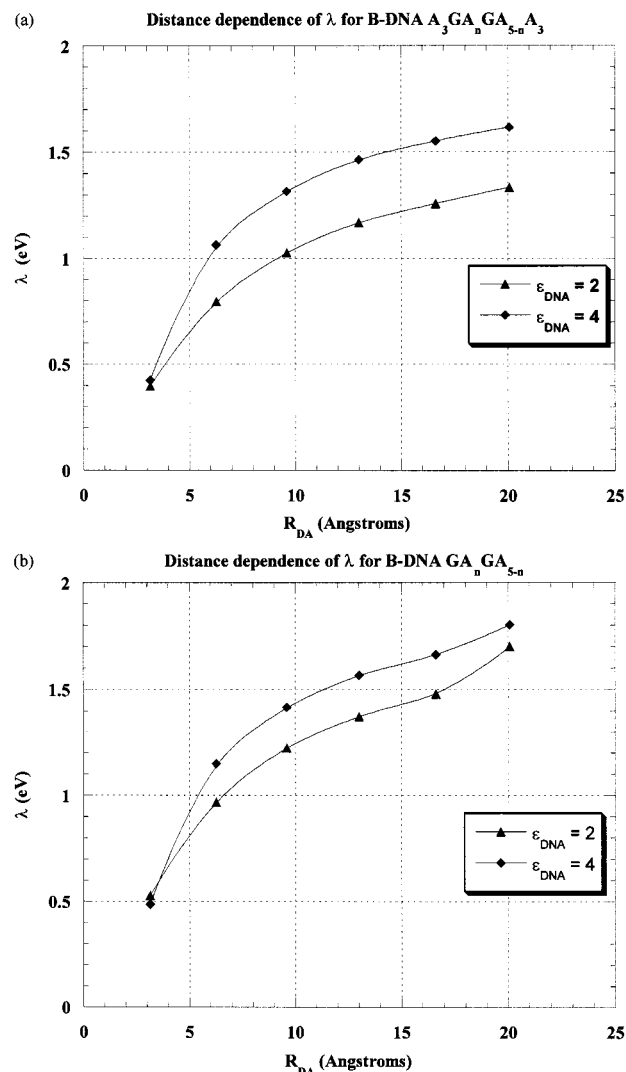


**Figure 5.** Calculated outer-sphere reorganization energies for guanine to guanine hole transfer in the B-DNA. (a) Guanine donor/acceptor groups are immersed in the helix; (b) one of the guanines is on the DNA strand end.

from the difference between the vertical (8.24 eV) and adiabatic (7.77 eV) IPs of guanine. Thus, the inner-sphere reorganization energy for hole transfer in GC/(AT) $_n$ /GC is roughly  $2 \times 0.47$  or 0.9 eV, and this further increases the tunneling energy gap.

The outer-sphere reorganization energy ( $\lambda_o$ ) grows with distance. Figure 5 shows the computed distance dependence of  $\lambda_o$  for (AT) $_m$ /GC/(AT) $_n$ /GC/(AT) $_m$  ( $n = 0-5$ ) in B-DNA;  $m$  was varied from 0 to 5 to simulate exposed or buried donor and acceptor groups. AT stacks were modeled with two choices of internal dielectric parameters,  $\epsilon_{DNA} = 2$  and 4. The solvent dielectric was set to 80. The computed  $\lambda_o$  values are larger (by about 0.1–0.2 eV) for the larger  $\epsilon_{DNA}$  value. The value of  $\lambda_o$  increases rapidly as a function of distance at short donor–acceptor distances and levels off at longer distances. The  $\lambda_o$  values for buried donors and acceptors ( $m = 5$ ) are smaller than the values for the exposed systems ( $m = 0$ ) by 0.07–0.37 eV, depending on how far the GC pair is from the solvent and the size of  $\epsilon_{DNA}$ . The computed values of the outer-sphere reorganization energies range from 0.4 eV (for neighboring GC base pairs) to 1.8 eV (5 bridging AT base pairs). A total reorganization energy in (GC)/(AT) $_n$ /(GC) (for  $n \geq 1$ ) is expected to be



larger than 2 eV and thus to shift the tunneling energy compared to gas-phase frozen geometry estimates by as much as 1 eV ( $\sim \lambda/2$ ).

The strong dependence of  $\lambda_o$  on distance computed here is consistent with earlier analysis of Tavernier and Fayer,<sup>102</sup> which used an integral expression for  $\lambda_o$ . It is important to point out that much of the theoretical analysis of DNA ET kinetics assumes distance independent reorganization energies. It is, of course, possible that these computations overestimate the distance dependence of  $\lambda_o$ . Possible sources of errors include delocalization of the donor or acceptor states onto the bridge or anomalously larger electronic polarizability for the DNA ET system (of particular concern are experiments involving excited states of donors or acceptors nearly degenerate with excited states of the bridge).

**Divide-and-Conquer Computations of  $H_{DA}$ .** All of the electronic coupling calculations described above use Hartree–Fock analysis. We also performed D&C calculations (see Appendix 2C) of  $H_{DA}$  in GC/(AT)<sub>n</sub>/GC and ZC/(AT)<sub>n</sub>/ZC to estimate the accuracy of the D&C method for DNA ET analysis. Results of these calculations appear in Figure 6. As the size of the fragments used to build the effective electronic Hamiltonian is increased, the computed  $H_{DA}$  values converge to those found in the full system calculations. For the ZC/(AT)<sub>n</sub>/ZC systems, we calculated  $\beta$  values of 1.69, 1.60, and 1.54 Å<sup>-1</sup> based on 2, 3, and 4 base pair fragmentation schemes, respectively. For the GC/(AT)<sub>n</sub>/GC system,  $\beta$  values of 1.34, 1.19, and 1.07 Å<sup>-1</sup> were obtained from 2, 3, and 4 base pair fragment-based calculations. Convergence of the D&C calculations with fragment size is more rapid for ZC/(AT)<sub>n</sub>/ZC than for GC/(AT)<sub>n</sub>/GC. Thus, ET systems with small tunneling energy gaps require larger fragments for accurate D&C computations of  $H_{DA}$ .

Figure 7 compares the tunneling energy dependence of  $H_{DA}$  in GC/(AT)<sub>3</sub>/GC obtained with effective Hamiltonians derived from 3 base pair Hartree–Fock calculations and “full” system calculations. These tunneling energy-dependence curves match very closely, indicating that the difference between “full” and D&C computations arises from errors in reproducing the tunneling energy gap, rather than from errors in omitting long-distance interactions in the D&C computations. Depending on the tunneling energy, the D&C method therefore gives reasonable estimates of  $\beta$  by using fragments of 4 base pairs. Thus, we can compute propagation through rather larger systems for a modest computational cost using the D&C approach.

**Influence of the Backbone and Basis Functions on Coupling through DNA.** The above calculations were all carried out on stacked base pairs without backbone. We now examine the influence of the DNA backbone on the computed electronic coupling matrix elements by performing calculations on GC/(AT)<sub>1</sub>/GC with and without the sugar–phosphate backbone. The phosphate was protonated in the calculations to give neutral structures. Results of these calculations appear in Table 1. Removal of the backbone does not produce significant changes in the coupling matrix elements.

Previous ab initio studies of DNA-mediated ET explored nearest-neighbor interactions between base pairs (no backbone). In those studies, standard split-valence basis sets (e.g., 6-31G\*) were found to be adequate.<sup>61,62</sup> To assess the importance of non-nearest neighbor interactions between bases (e.g., 1–3 interactions), we carried out calculations on single strand GAG stacks (also no backbone) using the 3-21G and 3-21++G basis sets (the latter basis set has diffuse basis functions on all atoms). The coupling matrix elements (computed using the energy

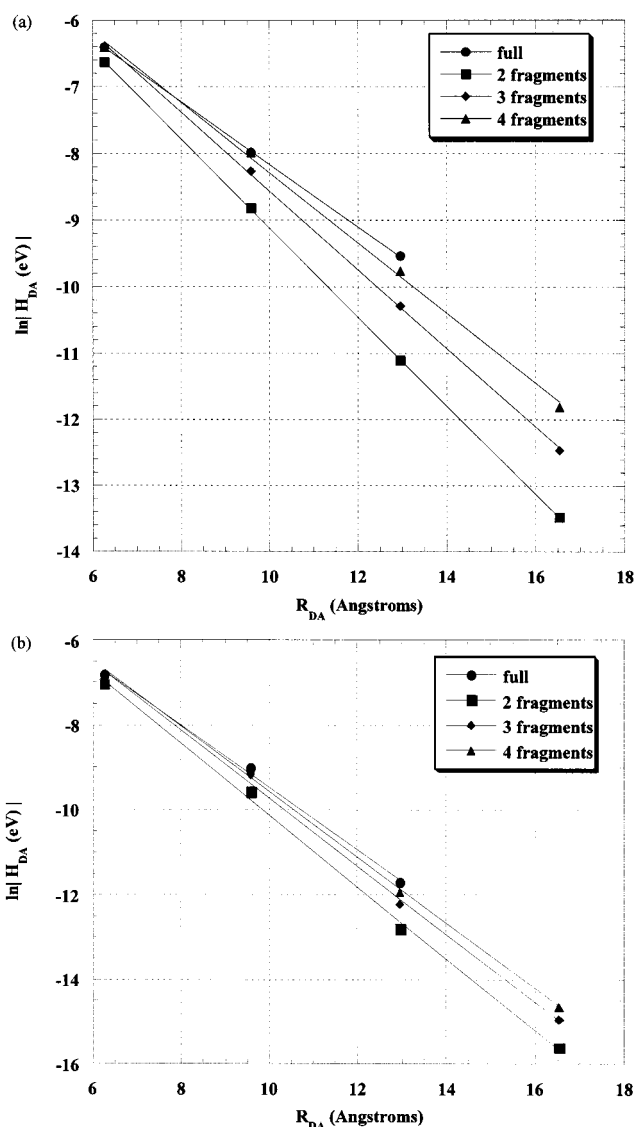


**Figure 6.** Comparison of D/A couplings for (a) GC/(AT)<sub>n</sub>/GC and (b) ZC/(AT)<sub>n</sub>/ZC. The “*n* fragment” notation refers to the size of the units (in base pairs) used to construct the composite molecule effective Hamiltonian in the D&C procedure. “full” means that no fragmentation was used.

splitting method) are 0.0416 and 0.0427 eV, respectively (less than a 3% difference). We conclude that split-valence basis sets without diffuse functions are adequate to calculate ET couplings in DNA stacks, in agreement with the previous analysis.<sup>61,62</sup>

**Condon Approximation for Small Tunneling-Energy Gaps.** In the regime of small tunneling-energy gaps,  $H_{DA}$  has a strong energy dependence and the Condon approximation may fail. To probe the validity of the Condon approximation, we computed  $k_{ET}^{non-ad}$  for GC/(AT)<sub>2</sub>/GC with  $H_{DA}(E)$  retained inside the integral of eq 2 (i.e., no Condon approximation) and compared this result with that calculated using eq 3. In the high-temperature regime ( $T = 298$  K), the removal and insertion spectral functions are

$$P_{remove}(E) = \left( \frac{1}{2\pi\lambda k_B T} \right)^{1/2} \exp \left[ -\frac{(E - E_D)^2}{2\lambda k_B T} \right] \quad (5a)$$

$$P_{insert}(E) = \left( \frac{1}{2\pi\lambda k_B T} \right)^{1/2} \exp \left[ -\frac{(E - E_A^+ - \lambda)^2}{2\lambda k_B T} \right] \quad (5b)$$

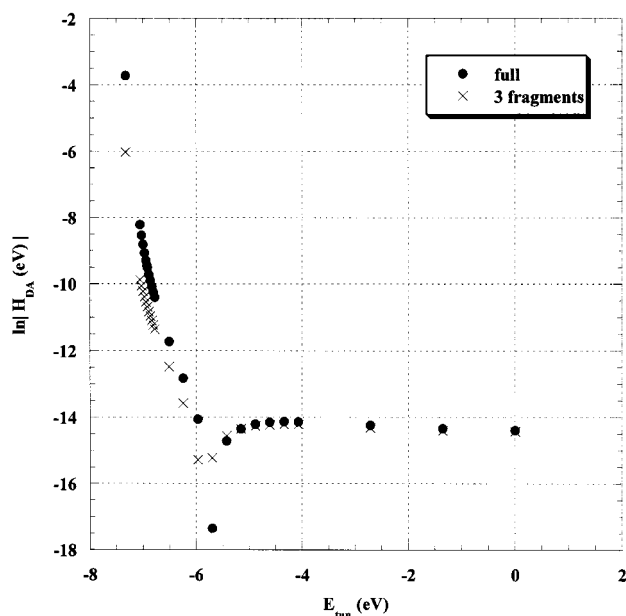


**Figure 7.** Comparison of the tunneling energy dependence of  $H_{DA}$  in GC/(AT)<sub>3</sub>/GC calculated with an effective Hamiltonian derived from full Hatree-Fock calculations and with an effective Hamiltonian obtained in divide-and-conquer technique using fragments of three bases.

**TABLE 1: Electronic Coupling Matrix Elements  $H_{DA}$  for GC/AT/GC with and without the Sugar–Phosphate Backbone**

method	$H_{DA}$ (without the backbone), eV	$H_{DA}$ (with the backbone), eV
minimum energy splitting	$5.59 \times 10^{-5}$	$6.66 \times 10^{-5}$
Green's Function	$5.84 \times 10^{-5}$	$6.43 \times 10^{-5}$

with  $E_A$  equal to the (negative) gas-phase ionization potential of the hole acceptor and  $E_D^+$  equal to the (negative) gas-phase electron affinity of the hole donor. Here,  $E_A = E_D^+ = -6.87$  eV.  $\lambda$  was taken equal to 1.3 eV (from outer-sphere reorganization energy calculations with  $\epsilon_{DNA} = 4$ ). The computed tunneling energy ( $E_t^{max}$ ) based on these energy parameters is  $-6.22$  eV, and  $H_{DA}(E_t^{max}) = -1.55 \times 10^{-3}$  eV. The rate calculated with the tunneling energy dependence of  $H_{DA}(E_t)$  included explicitly in eq 2 is  $1.3 \times 10^5$  s<sup>-1</sup>. This value is 20% larger than that calculated using  $H_{DA}(E_t^{max})$  and eq 3 (i.e., the Condon approximation), which gives a rate of  $1.1 \times 10^5$  s<sup>-1</sup>. Thus, the Condon approximation is valid for GC hole transport.

## V. Analysis of Experimental Systems

Our DNA ET analysis above focused on guanine oxidation reactions. These processes were studied extensively by the groups of Barton and Zewail,<sup>11,12</sup> Fukui and Tanaka,<sup>14,15</sup> Giese,<sup>17–19,21,23,103</sup> Lewis,<sup>27</sup> and Schuster.<sup>31–35,37–43</sup> The recent distance dependent kinetic studies of Barton and Zewail<sup>12</sup> and Lewis<sup>27,31,35</sup> and the ET product yield studies of Giese<sup>17–19,21,23</sup> indicate a  $\beta^r$ , rate decay exponents, of approximately  $0.6 \text{ \AA}^{-1}$ .<sup>12,17–19,21,23,27,31,59,103</sup> Studies of Tanaka and Fukui show an exponential decay constant more than twice this size,<sup>14,15,20</sup> while earlier studies of Barton reported a range of decay constants from  $0.1$  to  $1.0 \text{ \AA}^{-1}$ .<sup>9</sup> Recent experiments of Michel-Beyerle and co-workers report apparent  $\beta^r$  values larger than  $2 \text{ \AA}^{-1}$  but explain the large value as arising from a time-dependent excited-state relaxation process.<sup>14b</sup>

We focus our theoretical analysis on the studies of Lewis and co-workers<sup>31</sup> because of the range of distances probed and

the direct characterization of the charge transfer state. (Indeed, recent experiments of Barton and Zewail<sup>11,12</sup> and of Giese<sup>17–19,23,103</sup> are in qualitative agreement with these data.) The Lewis experiment probes photooxidation of guanine in a DNA hairpin structure with a stilbene (St) dicarboxamide bridge between oligonucleotide arms serving as the photooxidant. We compute nonadiabatic ET rates based on theoretical analysis of electronic couplings and reorganization energies for models of the DNA hairpin structures, and we compare the computed rates with the experimental data.

**Modeling the Stilbene DNA Hairpin Structures.** Recent structural data show that St positioning in the DNA hairpins is parallel to the base pairs.<sup>30</sup> We therefore expect that the St–GC coupling interactions will be similar to the GC–GC coupling interactions in GC/(AT)<sub>n</sub>/GC discussed in the previous section. We evaluate the validity of this assumption in Appendix 4.

The exact value for the reaction free energy of GC oxidation by St\* is unknown. St\* oxidizes G but not A. The redox potential difference of GC in an AT sequence and multiple AT's in a double helix is expected to be  $\sim 0.2$ – $0.4$  eV.<sup>124</sup> From these facts, we expect the free energy for the ET reaction between St\* and GC is  $\Delta G^\circ \sim -0.2$  eV. We computed the electron-transfer rate in St/(AT)<sub>n</sub>/GC using eq 1 with  $\Delta G^\circ = -0.2$  eV,  $\lambda$  computed using  $\epsilon_{DNA} = 4$  (1.1, 1.3, and 1.5 eV for  $n = 1, 2$ , and 3 respectively), and electronic couplings taken from GC/(AT)<sub>n</sub>/GC studies with the tunneling energy shifts equal to zero and  $\lambda/2$ . The computed ET rate constants are presented in Table 2.

The experimental ET rates often display an approximate exponential distance dependence that is characterized by a decay parameter  $\beta^r$ , where  $k_{ET} \propto \exp[-\beta^r R_{DA}]$ . It is important to note that the rate decay parameter ( $\beta^r$ ) and the  $|H_{DA}|^2$  decay parameter ( $\beta$ ) are different because  $\beta^r$  includes the distance dependence of  $\Delta G^\circ$  and  $\lambda$  in addition to the distance dependence of the coupling. The exponential decay constant that we computed for  $|H_{DA}|^2$  in GC/(AT)<sub>n</sub>/GC is about  $0.9 \text{ \AA}^{-1}$ , in apparent agreement with the experimental value of  $\beta^r \sim 0.7 \text{ \AA}^{-1}$ . However, Table 2 shows that when theoretical values of both the (distance dependent) reorganization energies and the coupling matrix elements are used in the rate equation (eq 1), the predicted value of  $\beta^r$  is much larger ( $\sim 1.5 \text{ \AA}^{-1}$  [without the shift],  $2.5 \text{ \AA}^{-1}$  [with the shift]) than experimentally observed. The difference between computed and observed rates for long distance hole transfer is quite dramatic: approximately 5–8 orders of magnitude for  $n = 3$ . This dramatic discrepancy is unlikely to arise from inaccuracy of the theoretical models used for computation of the donor/acceptor electronic couplings and reorganization energies, as these methods are reliable for numerous other ET systems. Thus, we conclude that the single-step nonadiabatic ET mechanism is probably not operative, at least for ET across three or more base pairs. Therefore, we conclude that guanine oxidation proceeds in these systems by some other physical mechanism. A possible mechanism that explains long-range hole transfer in DNA is thermally activated hole hopping.<sup>11,47,49,50,59,65</sup> For this hopping mechanism to be viable, the AT bridge localized states should be thermally accessible on the time scale of the St excited state. As we discussed above, the redox potential of St\* is somewhere between the redox potential of the pure (AT)<sub>n</sub> sequence and the redox potential of GC inside of an AT run. The gap between the GC and the AT run redox potentials is just  $0.2$ – $0.4$  eV. One therefore expects that the hole transfer from the (AT)<sub>n</sub> bridge to St\* is only slightly uphill, with  $\Delta G^0 \sim +0.1$  to  $+0.2$  eV.

TABLE 2: Hole-Transfer Rate Constant<sup>a</sup>

number of AT base pairs	$k_{\text{ET}}$ (experimental), $\text{s}^{-1}$	$k_{\text{ET}}$ (theoretical, without energy shift), $\text{s}^{-1}$	$k_{\text{ET}}$ (theoretical, with energy shift), $\text{s}^{-1}$
1		$2.1 \times 10^{10}$	$6.1 \times 10^9$
2	$2.6 \times 10^{11}$	$1.2 \times 10^8$	$3.2 \times 10^6$
3	$3.2 \times 10^{10}$	$6.8 \times 10^5$	$3.5 \times 10^2$
4	$1.7 \times 10^9$		
5	$2.1 \times 10^8$		

<sup>a</sup> The experimental values are from ref 31. The rheoretical values are obtained from  $H_{\text{DA}}$  of GC/(AT)<sub>*n*</sub>/GC using eq 1 with  $\lambda$  at  $\epsilon_{\text{DNA}} = 4$ .

## VI. Discussion

In this paper, we attempted to perform a comprehensive quantitative theoretical analysis of electron (hole) tunneling in DNA. The physical aspect of the problem that received central attention was the tunneling energy dependence of the donor–acceptor coupling. In typical cases of electron (hole) transfer in DNA, donor, acceptor, and bridge-localized states are separated by free-energy gaps of just a few tenths of an electronvolt. As a consequence, we conclude that the dependence of the electronic coupling on the tunneling energy gap is very steep. Therefore, quantitative estimates of the tunneling energy gap for DNA ET is critical for meaningful electronic-coupling computations. Details of the donor–acceptor electronic structure were found to be of limited importance. Once reliable estimates of the tunneling energy gaps are made, reasonable values of the electronic couplings can be found from computations on simple model ET systems such as GC/(AT)<sub>*n*</sub>/GC. Our analysis showed a critical influence of the vibronic coupling ( $\lambda$ ) on the value of the tunneling energy gap. We showed that the average tunneling energy gap is increased by about half the value of the ET reorganization energy ( $\sim \lambda/2$ ). For G oxidation, this shift of the tunneling-energy gap results in a dramatic increase in the computed exponential decay constant for the electronic coupling and the ET rate. A similar  $\lambda$ -dependent coupling expression has been used in the past.<sup>59,86,88</sup>

We computed the distance dependence of the outer-sphere reorganization energy for GC oxidation using continuum electrostatics methods. These methods take into account the actual three-dimensional shape of the DNA molecule. We found, in agreement with other theoretical studies, that the reorganization energy for GC oxidation increases rapidly with distance. Taking the rapid distance dependence of the coupling and reorganization energy into account, the rates of nonadiabatic DNA ET are predicted to decay very rapidly with distance;  $\beta^r$  values of  $\sim 1.5$ – $2.5 \text{ \AA}^{-1}$  are calculated. These predicted  $\beta^r$  values for the superexchange mechanism are much larger than observed experimentally. We conclude, therefore, that switching of the ET mechanism takes place for more than two bridging AT base pairs. A possible ET mechanism for the longer distance ET is thermally activated hopping.

We have explored several methods to calculate the donor/acceptor electronic coupling. A new Green's function approach was compared to energy splitting methods and was found to be accurate and efficient for these DNA systems. The perturbation approach was found to reproduce the electronic coupling values computed with energy splitting and Green's function methods and allows access to different tunneling energy gaps.

We investigated the validity of a divide-and-conquer approach for the computation of ET couplings in DNA. We find convergence of the D&C method in terms of the size of the fragments is faster for larger tunneling energy gaps. We also find that even small fragment calculations (2–3 base pairs per fragment) reproduce the results of full calculations if the tunneling energy gap is set to the right value.

The tunneling energy gap in ET systems fluctuates, due to the donor, acceptor, and bridge energy fluctuations. We have tested the validity of the Condon approximation which uses an average tunneling energy gap in donor/acceptor calculations (instead of explicitly integrating  $|H_{\text{DA}}|^2$  over the tunneling energy gap). The Condon approximation (as defined above) was found to be adequate for hole transfer in DNA.

Theoretical methods used in this paper, although expected to give reliable estimates of DNA ET parameters, are certainly limited. Our analysis neglects a number of effects that may influence computed DNA ET rates. The electronic structure methods used here are limited by the absence of electron correlation. Correlation effects are found to be of modest importance for ET in many bridged systems. In the case of DNA ET, correlation effects may be more pronounced because of the small tunneling energy gaps. There are approaches to introduce correlation effects to the electron-transfer problem. For example, Dyson equation approaches to correlation have been used to compute ionization potentials and electron affinities of DNA bases.<sup>125</sup> Ideally, the electronic structure analysis should be performed on the ET transition state, which involves nonequilibrium DNA structure and solvation. As such, coupled molecular mechanics and electronic structure theory may be needed to access these structures.

Another limitation of the present studies is the analysis of a single idealized geometry (canonical B-DNA). The coupling element,  $H_{\text{DA}}$ , should be averaged over rapid structural fluctuations when computing the ET rate.<sup>61</sup> These fluctuations can be particularly important if parallel pathways tend to be destructive in their interferences.<sup>105,106</sup> Our limited analysis of alternative geometries does not indicate a hypersensitivity to geometry, but this issue remains open.

**Comparison of Electron Tunneling in DNA and in Proteins.** The importance of electron transfer in proteins has long been recognized, and these reactions have been intensively studied both experimentally and theoretically.<sup>107–111</sup> It is important to identify the principle similarities and differences between electron tunneling in DNA and proteins.

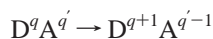
Typical biological donor and acceptor cofactors have redox potentials in the range of  $-1.0$  to  $+1.0 \text{ V}$  versus the normal hydrogen electrode and are energetically well separated from the oxidation and reduction potentials of the protein (although protein electron transfer can involve ET to aromatic amino acids, as in ribonucleotide reductase, cytochrome *c* peroxidase, and cytochrome P-450<sup>112–115</sup>). The success of theoretical models for protein ET is largely due to the substantial energetic separation of protein redox cofactors and mediating amino acid bridging groups (more than 1 eV) resulting in approximately universal values for effective tunneling barriers for specific classes of protein contacts (bonded, H-bonded, through space). This relative simplicity allows a qualitative description of electron tunneling in proteins with simple tunneling models.<sup>107,108</sup> The situation in DNA ET is made more complex by



the small tunneling energy gap for hole transfer among native and modified bases.

### Appendix 1: Tunneling energy and electron insertion/removal functions

We describe here the spectral functions associated with the reaction



We show first that these functions are Gaussian with peak separation of  $\lambda + \Delta G^\circ$ . We then describe how these functions are associated with gas-phase electronic structure calculations.

Gas-phase calculations of donor/acceptor electronic structure ignore the explicit effects of solvent and bridge polarization on the tunneling energy. The shifts in the energies of the charged donor and acceptor states due to polarization of the medium are expected to be large, on the order of 1 eV. Changes in tunneling energy gaps as large as this can dramatically influence calculated donor/acceptor electronic interactions. The analysis that follows provides an estimate of environment effects on the tunneling energy gap for hole transfer between two guanine bases.

The energy of the electron donor,  $E_D(Q)$ , is defined as minus the energy needed to remove an electron from the donor at a given nuclear configuration  $Q$ . The energy of the electron acceptor,  $E_A(Q)$ , is defined as the (negative) binding energy of the acceptor at the nuclear configuration  $Q$  with the electron absent from the donor. In the activated complex,  $E_D(Q) = E_A(Q) = E_{\text{tun}}$ .  $E_{\text{tun}}$  is the electron tunneling energy.

Depending upon whether the electron is on the donor, acceptor, or removed from the system altogether ("vac"), the nuclear Hamiltonian is  $H_D(Q)$ ,  $H_A(Q)$ , or  $H_{\text{vac}}(Q)$ , respectively:

$$H_D(Q) = H_{\text{vac}}(Q) + E_D(Q) \quad (\text{A1a})$$

$$H_A(Q) = H_{\text{vac}}(Q) + E_A(Q) \quad (\text{A1b})$$

$\langle E_D \rangle_D$ ,  $\langle E_D \rangle_A$ , and  $\langle E_D \rangle_{\text{vac}}$  are the average electronic energies for nuclear Hamiltonians  $H_D(Q)$ ,  $H_A(Q)$ , and  $H_{\text{vac}}(Q)$  with the electron placed on the donor.  $\langle E_A \rangle_D$ ,  $\langle E_A \rangle_A$ , and  $\langle E_A \rangle_{\text{vac}}$  are defined as the respective averages of the binding energies when the electron is placed on the acceptor.

The parameter  $\eta$  is now introduced to the Hamiltonian,  $H^\eta(Q)$ , to change it smoothly from  $H_{\text{vac}}(Q)$  to  $H_D(Q)$  as  $\eta$  changes from 0 to 1:

$$H^\eta(Q) = H_{\text{vac}}(Q) + \eta E_D(Q) \quad (\text{A2})$$

The binding energy averages can be computed for any specific values of  $\eta$ :

$$\langle E_D \rangle_\eta = \frac{\int dQ E_D(Q) \exp(-H^\eta(Q)/k_B T)}{\int \exp(-H^\eta(Q)/k_B T) dQ} \quad (\text{A3})$$

and the derivative of this function versus  $\eta$  is

$$\frac{\partial}{\partial \eta} \langle E_D \rangle_\eta = -\frac{1}{k_B T} \left( \frac{\int dQ E_D^2(Q) \exp(-H^\eta(Q)/k_B T)}{\int \exp(-H^\eta(Q)/k_B T) dQ} - \left( \frac{\int dQ E_D(Q) \exp(-H^\eta(Q)/k_B T)}{\int \exp(-H^\eta(Q)/k_B T) dQ} \right)^2 \right) \quad (\text{A4a})$$

$$\frac{\partial}{\partial \eta} \langle E_D \rangle_\eta = \frac{1}{k_B T} (\langle E_D \rangle_\eta^2 - \langle E_D^2 \rangle_\eta) = \frac{1}{k_B T} \langle \Delta E_D^2 \rangle_\eta \quad (\text{A4b})$$

Assuming that the average of  $E_D(Q)$  responds linearly to the changes in the nuclear Hamiltonian:

$$\langle E_D \rangle_{\text{vac}} - \langle E_D \rangle_D = \frac{1}{k_B T} \langle \Delta E_D^2 \rangle \quad (\text{A5a})$$

Similarly

$$\langle E_A \rangle_{\text{vac}} - \langle E_A \rangle_A = \frac{1}{k_B T} \langle \Delta E_A^2 \rangle \quad (\text{A5b})$$

Because the right sides of the above equations are always positive, the solvated-species energies lie below the vacuum levels so  $\langle E_D \rangle_D < \langle E_D \rangle_{\text{vac}}$  and  $\langle E_A \rangle_A < \langle E_A \rangle_{\text{vac}}$ . Disregarding the influence of one redox center on the other,  $\langle E_D \rangle_{\text{vac}} = \langle E_D \rangle_A$  and  $\langle E_A \rangle_{\text{vac}} = \langle E_A \rangle_D$ . Fluctuations of binding energies now can be expressed through the ET reorganization energy  $\lambda$ :

$$\frac{1}{k_B T} \langle \Delta E_D^2 \rangle = \langle E_D \rangle_A - \langle E_D \rangle_D = \lambda \quad (\text{A6a})$$

$$\frac{1}{k_B T} \langle \Delta E_A^2 \rangle = \langle E_A \rangle_D - \langle E_A \rangle_A = \lambda \quad (\text{A6b})$$

The probability distribution of the electron binding energy  $E_D$  is estimated by computing the work need to change the Hamiltonian  $H^\eta(Q)$  from the state  $\eta = 1$  to  $\eta = \eta_0$ :

$$\Delta A = \int_1^{\eta_0} (\langle E_D \rangle_{\text{vac}} - \langle E_D \rangle_D) (1 - \eta) d\eta \quad (\text{A7a})$$

$$\Delta A = \frac{1}{2} (\langle E_D \rangle_{\text{vac}} - \langle E_D \rangle_D) (1 - \eta_0)^2 \quad (\text{A7b})$$

$$\Delta A_\eta = \frac{1}{2} (\langle E_D \rangle_{\text{vac}} - \langle E_D \rangle_D) \left( \frac{\langle E_D \rangle'_\eta - \langle E_D \rangle_D}{\langle E_D \rangle_{\text{vac}} - \langle E_D \rangle_D} \right)^2 = \frac{(\langle E_D \rangle'_\eta - \langle E_D \rangle_D)^2}{2(\langle E_D \rangle_{\text{vac}} - \langle E_D \rangle_D)} = \frac{(\langle E_D \rangle'_\eta - \langle E_D \rangle_D)^2}{2\lambda} \quad (\text{A8})$$

The probability distribution of  $E_D$  is therefore Gaussian:

$$p(E_D) \sim \exp\left(-\frac{(\langle E_D \rangle'_\eta - \langle E_D \rangle_D)^2}{2\lambda k_B T}\right) \quad (\text{A9})$$

Gaussian probability distributions of binding energies  $E_D$  and  $E_A$  in donor and acceptor states are schematically represented in Figure 1.

For neutral molecules in solution, the average electrostatic potential created by the solvent is close to zero. Therefore, for ET reactions between neutral guanine and guanine radical cation, the average binding energies  $\langle E_D \rangle_D$  and  $\langle E_A \rangle_A$  should be close to their (negative) ionization potentials in vacuum. The tunneling energy distribution corresponds to the overlap of the distributions of  $E_D$  in the donor state and  $E_A$  in the acceptor



state. The peak of this distribution occurs at

$$E_T = \frac{1}{2} (\langle E_D \rangle_A + \langle E_D \rangle_D) = \frac{1}{2} (\langle E_A \rangle_A + \langle E_A \rangle_D)$$

or  $\lambda/2$  above  $\langle E_D \rangle_D$  and  $\langle E_A \rangle_A$ .

For the donor and acceptor species that are charged in their reduced state, the solvent will create an average electrostatic potential that will be positive for negatively charged molecules and negative for positively charged molecules. This electrostatic potential will produce a shift of  $\langle E_D \rangle_D$  and  $\langle E_A \rangle_A$  from the vacuum electronic binding energies.

## Appendix 2: Computing Donor–Acceptor Coupling Interactions

**A. Energy Splitting.** The effective donor–acceptor interaction,  $H_{DA}$  (eq 1), can be computed in several ways for multielectron molecular wave functions. The ET event occurs, within the Condon approximation, in a system configuration where donor- and acceptor-localized electronic states ( $\varphi_D$  and  $\varphi_A$ ) are mixed by bridge mediated superexchange interactions. In this activated state, the system is quasidegenerate, with the lowest energy eigenstates approximately  $\Psi_0 = 1/\sqrt{2} (\varphi_D + \varphi_A)$  and  $\Psi_1 = 1/\sqrt{2} (\varphi_D - \varphi_A)$ . One can compute  $H_{DA}$  as half of the energy splitting between the energies of these two electronic eigenstates:<sup>94</sup>

$$H_{DA} = \frac{1}{2} |E_0 - E_1| \quad (A10)$$

The calculations of  $H_{DA}$  in this paper are performed using ground-state Hartree–Fock methods and Koopmans’ theorem.<sup>94</sup> Koopmans’ theorem states that the energies of occupied and unoccupied Hartree–Fock molecular orbitals for a closed-shell system approximate the (negative) vertical ionization potentials ( $-IP$ ) and electron affinities ( $-EA$ ), respectively. To calculate  $H_{DA}$ , we perform Hartree–Fock calculations on model ET systems with an “additional” electron. In the Koopmans’ theorem approach, the energy difference between the HOMO ( $E_{HOMO}$ ) and the next-highest occupied molecular orbital ( $E_{HOMO-1}$ ) approximates the energy difference between the two quasi-degenerate electronic eigenstates of the ET system (eq A11). From Koopmans’ theorem:

$$\begin{aligned} -E_{HOMO} &= IP_1 = E_0^{Ne} - E_0^{(N+1)e} \\ -E_{HOMO-1} &= IP_2 = E_1^{Ne} - E_0^{(N+1)e} \\ -(E_{HOMO} - E_{HOMO-1}) &= -E_0^{Ne} + E_1^{Ne} = 2|H_{DA}| \quad (A11) \end{aligned}$$

where  $E_0^{Ne}$  and  $E_1^{Ne}$  are the energies of the quasi-degenerate ground and first-excited electronic states of the electron-transfer system.  $E_0^{(N+1)e}$  is the ground-state energy of the system with an extra electron. Thus in the Koopmans’ theorem approximation, the donor–acceptor interaction equals one-half the difference between the two highest-occupied molecular orbitals of the system with an extra electron.<sup>94,116</sup> This approach is used in many theoretical studies of ET.<sup>117,118</sup>

The DNA systems that we consider are of low symmetry, and in general, the computed ET system will not be in the activated state (donor and acceptor states will have different energies). A simple way to drive the system to this point is to apply an electric field along the donor–acceptor axis, modifying the effective Hamiltonian by<sup>95–97</sup>

$$\mathbf{H}'(\epsilon_{DA}) = \mathbf{H}_{\text{eff}}(0) + [\mathbf{d}_x e_x + \mathbf{d}_y e_y + \mathbf{d}_z e_z] \epsilon_{DA} \quad (A12)$$

where  $e_x$ ,  $e_y$ , and  $e_z$  are components of the unit vector directed from donor to acceptor;  $\mathbf{d}_x$ ,  $\mathbf{d}_y$ , and  $\mathbf{d}_z$  are the electric dipole matrices in the basis of active orbitals; and  $\epsilon_{DA}$  is the electric field strength. The donor–acceptor splitting as a function of field strength passes through a minimum. We compute  $H_{DA}$  as one-half of the minimum value of this energy splitting.

**B. Green’s Function and Perturbation Analysis.** The energy splitting approach to  $H_{DA}$  is costly because it requires repeated diagonalization of a large effective Hamiltonian. An alternative approach is to reduce the effective Hamiltonian to a two-level system prior to diagonalizing. This approach is less costly and equally effective for most of the DNA systems of interest here. If the approximate donor and acceptor localized electronic states ( $|D\rangle$  and  $|A\rangle$ ) are known, an effective  $2 \times 2$  Hamiltonian describing the quasi-degenerate eigenstates of the system can be obtained from the  $2 \times 2$  Green’s Function matrix calculated for these states:<sup>98</sup>

$$\begin{pmatrix} H_{DD}^{\text{eff}}(E) & H_{DA}^{\text{eff}}(E) \\ H_{AD}^{\text{eff}}(E) & H_{AA}^{\text{eff}}(E) \end{pmatrix} = E \begin{pmatrix} S_{DD} & S_{DA} \\ S_{AD} & S_{AA} \end{pmatrix} - \begin{pmatrix} S_{DD} & S_{DA} \\ S_{AD} & S_{AA} \end{pmatrix} \begin{pmatrix} G_{DD}(E) & G_{DA}(E) \\ G_{AD}(E) & G_{AA}(E) \end{pmatrix}^{-1} \begin{pmatrix} S_{DD} & S_{DA} \\ S_{AD} & S_{AA} \end{pmatrix} \quad (A13)$$

In this equation, we must choose donor and acceptor states, represented by expansion coefficient vectors  $c_D$  and  $c_A$ . As such, the elements of the above  $2 \times 2$  equation are  $\mathbf{G}_{nm} = \mathbf{c}_n + \mathbf{G}\mathbf{c}_m$  ( $\mathbf{G}$  is the energy dependent Green’s function matrix for the full system),  $n = D$  or  $A$ ,  $m = D$  or  $A$ , and  $\mathbf{S}_{nm} = \mathbf{c}_n + \mathbf{c}_m$ . The Green’s function matrix is computed using the Fock matrix of the full system, and  $\hat{G} = (E - \hat{F})^{-1}$ . This expression for the  $2 \times 2$  effective Hamiltonian is equivalent to the one developed earlier using a projection operator (partitioning) technique.<sup>119</sup>

The effective Hamiltonian defined by eq A13 has exactly the same energy eigenvalue spectrum as the total electronic Hamiltonian for the system. However, its matrix elements of the effective Hamiltonian are energy dependent. To compute  $H_{DA}$ , the donor and acceptor electronic states  $|D\rangle$  and  $|A\rangle$  are defined by truncating the molecular orbitals located mostly on the donor or those located mostly on the acceptor. The orbital truncation is performed by setting to zero expansion coefficients for the atomic orbitals that do not lie on donor or acceptor atoms. In the case of hole transfer between GC base pairs, the donor and acceptor states are chosen to be the highest lying G molecular orbitals, truncated to include amplitude only on the atoms of the guanine.

The Green’s function matrix elements involving D and A states are found using

$$\mathbf{G} = \mathbf{S}(\mathbf{E}\mathbf{S} - \mathbf{H})^{-1}\mathbf{S} \quad (A14)$$

The tunneling energy,  $E_T$ , for the calculation of the Green’s function matrix elements is set to the average of the donor and acceptor molecular orbital energies obtained from the Hartree–Fock calculations of the whole system (although they can be derived from calculation on the isolated donor and acceptor groups).  $H_{DA}$  is just the off-diagonal element on the left-hand side of eq A13.

A third method to compute  $H_{DA}$  uses Löwdin reduction,<sup>120</sup> or Brillouin–Wigner perturbation theory. For the donor and acceptor localized orbitals  $|D\rangle$  and  $|A\rangle$  (defined above), the electronic coupling between them is

$$H_{DA}(E) = \mathbf{D}^+(\mathbf{E}\mathbf{S}_{DB} - \mathbf{H}_{DB})(\mathbf{E}\mathbf{S}_B - \mathbf{H}_B)^{-1}(\mathbf{E}\mathbf{S}_{AB} - \mathbf{H}_{AB})\mathbf{A} \quad (A15)$$

The elements on the right-hand side of this equation are  $N \times 1$ ,  $N \times M$ ,  $M \times M$ ,  $M \times P$ , and  $1 \times P$ , respectively. The donor consists of  $N$  orbitals, the bridge consists of  $M$  orbitals, and the acceptor consists of  $P$  orbitals. This formulation is particularly convenient because it allows one to analyze the tunneling-energy dependence of bridge propagation by analyzing  $(ES_B - H_B)^{-1}$  for different values of  $E$ .

For electron-transfer involving guanine bases considered in this paper, Green's function and perturbation methods reproduced well (accuracy of about 10%) the values of the ET couplings obtained with the energy-splitting method.

**C. Divide-and-Conquer Analysis.** In the previous sections, we described methods to compute  $H_{DA}$  using Hartree–Fock/Koopmans' theorem methods. For large systems, Hartree–Fock calculations are inaccessible. We have addressed this challenge by developing a “divide-and-conquer” scheme to construct the one-electron effective Hamiltonian (Fock matrix) for large ET systems based on ab initio fragment calculations.<sup>119</sup> The approach pieces together an approximation to the Fock matrix from the fragment calculations. The following steps are taken in the calculation: (1) the system is divided into overlapping fragments and Hartree–Fock calculations are performed on each fragment. The effective Hamiltonian matrix of the whole system is pieced together from the sub-matrices of these fragments. For fragments, we build the Fock matrices in a basis of valence orbitals (the P-space) using

$$H_{pp}^{\text{eff}}(E) = ES_{pp} - S_{pp}G_{pp}^{-1}(E)S_{pp} \quad (\text{A16})$$

This approach generates the electronic propagation characteristics of the valence orbitals (contained in  $G$ ) that arise from a much larger basis-set calculation. To discriminate between sub-matrices of the effective Hamiltonian from the different fragments, we employ a “protection-number” scheme. The system and fragments are sub-divided into atomic groups that correspond roughly to chemical functional groups. Each group in a fragment is assigned a protection number from 0 to 1, indicating how much that group is perturbed by the fragmentation compared to the uncut structure. A value of 1 corresponds to the unperturbed structure. The closer the chemical group is to the point at which a “cut” is made, the smaller its protection value. The protection values for the groups were set manually for the computations described in the paper (the guanine base closest to the “cut” gets a protection number 0.2, the base separated by 1 base from the “cut” get a protection number  $0.2^{1/2}$ , the next one receives a protection number  $0.2^{1/3}$ , and so on. When the composite Hamiltonian is built from the fragment sub-matrices, matrix elements between groups are taken from calculations that have the largest product of protection values for the two groups. Electronic coupling calculations using this composite effective Hamiltonian (or effective Fock matrix) were performed just as calculations would that did not rely on the fragmentation approach.

### Appendix 3: Reorganization Energy Calculations

We used finite-difference solutions of the Poisson equation to estimate outer-sphere reorganization energies. The computational scheme is similar to those previously described.<sup>121,122</sup> We distribute a +1e charge on the non-hydrogen donor atoms and a −1e charge on the non-hydrogen acceptor atoms. This charge distribution approximates changes in the electron density associated with ET. Two finite-difference Poisson calculations of electrostatic potentials are then performed. One calculation employs a uniform high-frequency dielectric constant ( $\epsilon_\infty = 2.0$ ),

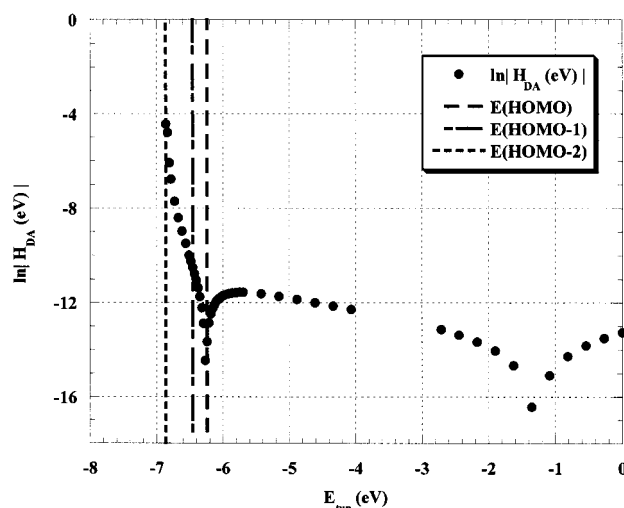


**Figure A1.** Tunneling energy dependence of  $H_{DA}$  for St/(AT)<sub>2</sub>/GC with −0.02e added to each heavy atom of stilbene.

modeling the electronic polarization response to ET. A second calculation selects a low-frequency dielectric constant inside DNA ( $\epsilon^{\text{DNA}}$ ) equal to 2 or 4 and a low-frequency dielectric for the solvent ( $\epsilon^{\text{water}}$ ) of 81. The outer-sphere reorganization energies are computed as the difference of the total electrostatic energies of the system obtained in those two calculations. As in other finite-difference molecular electrostatic analysis, the boundary between the molecule and the solvent is determined by the explicit three-dimensional structure of the solute molecule (here DNA).<sup>101,121</sup>

### Appendix 4: St–GC Coupling Calculations

To test the validity of the assumption that St–GC coupling can be approximated by GC–GC coupling, we examined St/(AT)<sub>2</sub>/GC systems and explored the influence of the St acceptor electronic structure and position on the coupling. In a simple orbital description of ET in the DNA hairpins, an electron transfers from the HOMO of guanine to the orbital associated with the HOMO of the ground-state stilbene. We computed ET couplings in GC/(AT)<sub>n</sub>/St from the energy splitting between the highest occupied orbitals localized on guanine and stilbene. To construct models for the GC/(AT)<sub>n</sub>/St structures, we first build GC/(AT)<sub>n</sub> stacks (no sugar–phosphate backbone) in the canonical B-DNA geometry. We then place a dicarboxamide St molecule in van der Waals contact with the AT stack. The St plane is parallel to the DNA base planes and its  $C_2$  symmetry axis coincides approximately with the DNA helical axis. Ground-state Hartree–Fock calculations on this structure revealed that the St HOMO falls below the AT-localized highest occupied orbital. In the experiment, St does not oxidize the (AT)<sub>n</sub> stack. Therefore, we believe the computed MO energy ordering is an artifact of the simplified orbital modeling of the St excited state. To correct the energy ordering, we added negative point charges (−0.02e) to the stilbene heavy atoms. As a result, the St HOMO appeared higher in energy by 0.6 eV compared to the highest energy AT localized orbitals. The magnitude of the St to GC coupling in GC/(AT)<sub>2</sub>/St was computed to be  $10^{-6}$  eV, a value much smaller than the ET coupling in the GC/(AT)<sub>2</sub>/GC structure. To understand the physical origin of this result, we compared the  $H_{DA}$  tunneling energy dependence in St/(AT)<sub>2</sub>/GC and GC/(AT)<sub>2</sub>/GC. (Figures A1 and A2, respectively).  $H_{DA}$  varies smoothly with tunneling energy for GC/(AT)<sub>2</sub>/GC in the regime of energies close to the GC base pair HOMO energy. However, in the St/(AT)<sub>2</sub>/GC

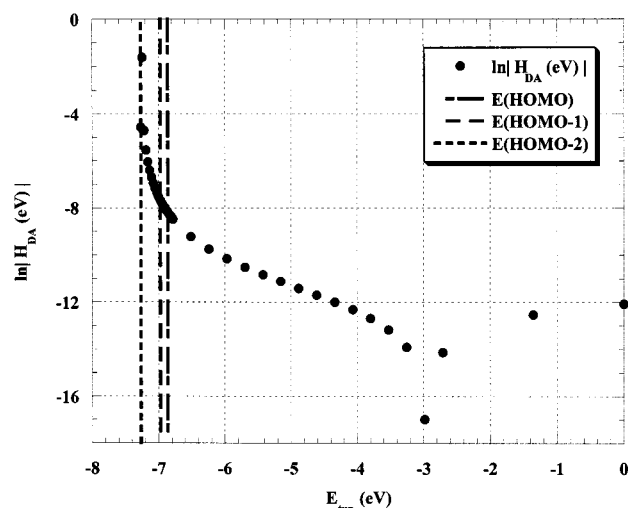


Figure A2. Tunneling energy dependence of  $H_{DA}$  in GC/(AT)<sub>2</sub>/GC.

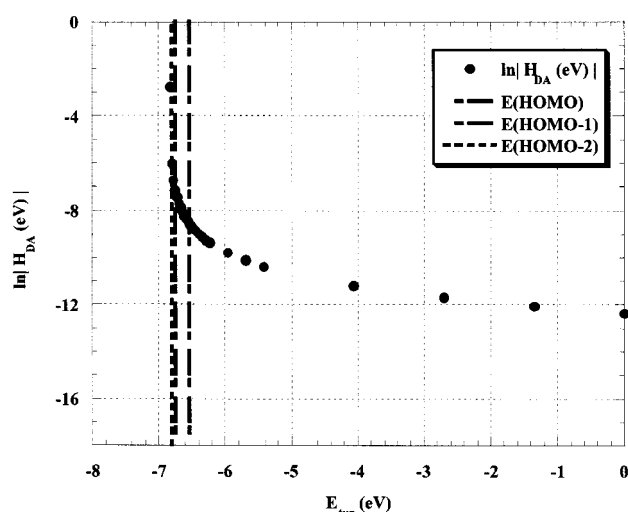


Figure A3. Tunneling energy dependence of  $H_{DA}$  for St/(AT)<sub>2</sub>/GC with St rotated by 10° about the  $C_2$  axis with  $-0.03e$  added to each heavy atom of the St and  $+0.015e$  on AT adjacent to St.

structures, there is a “dip” in the tunneling energy dependence of  $H_{DA}$  near the GC base pair HOMO energy. Dips of this kind are observed in hydrocarbon spacers and in peptides.<sup>99,106,123</sup> The dips arise from interferences among multiple tunneling pathways, and can be hypersensitive to geometry. This interference is probably the cause of the exceptionally small coupling matrix element computed for the St systems. (Dips in  $H_{DA}$  also occurred in calculations of  $H_{DA}$  in A-form GC/(AT)<sub>2</sub>/GC at tunneling energies corresponding to GC and ZC energies.) Geometry sampling is particularly important in instances where these pathways interfere.<sup>106</sup> We rotated St by 10° about its  $C_2$ -axis with  $-0.03e$  and  $+0.015e$  charges added to each heavy atom of St and AT base pair adjacent to the St, respectively. We found  $H_{DA}$  coupling values of the same order of magnitude as for the GC/(AT)<sub>2</sub>/GC structure. The tunneling energy dependence (Figure A3) is smooth in the vicinity of the GC localized orbital energies in this St/(AT)<sub>2</sub>/GC structure. We believe that the conformations with strongest donor–acceptor couplings will dominate the ET process in these somewhat flexible structures. For St/(AT)<sub>2</sub>/GC we believe, therefore, that the larger coupling value, which is similar to the coupling value for GC/(AT)<sub>2</sub>/GC, is the most relevant one to use in nonadiabatic rate calculations (thermal averaging, of course, should be carried out more rigorously to obtain more accurate results). In

summary, we conclude that GC/(AT)<sub>n</sub>/GC structures provide a reasonable approximate model for studies of ET interactions in the St/(AT)<sub>n</sub>/GC systems.

**Acknowledgment.** We thank NIH (GM57876) for support of this research and F.D. Lewis for helpful discussions.

## References and Notes

- (1) Murphy, C. J.; Arkin, M. R.; Jenkins, Y.; Ghatlia, N. D.; Bossmann, S. H.; Turro, N. J.; Barton, J. K. *Science* **1993**, 262, 1025–1029.
- (2) Murphy, C. J.; Arkin, M. R.; Ghatlia, N. D.; Bossmann, S.; Turro, N. J.; Barton, J. K. *Proc. Natl. Acad. Sci. U.S.A.* **1994**, 91, 5315–5319.
- (3) Arkin, M. R.; Stemp, E. D. A.; Holmlin, R. E.; Barton, J. K.; Hormann, A.; Olson, E. J. C.; Barbara, P. F. *Science* **1996**, 273, 475–480.
- (4) Hall, D. B.; Holmlin, R. E.; Barton, J. K. *Nature* **1996**, 382, 731–735.
- (5) Dandliker, P. J.; Holmlin, R. E.; Barton, J. K. *Science* **1997**, 275, 1465–1468.
- (6) Holmlin, R. E.; Dandliker, P. J.; Barton, J. K. *Angew. Chem., Int. Ed. Engl.* **1997**, 36, 2715–2730.
- (7) Kelley, S. O.; Holmlin, R. E.; Stemp, E. D. A.; Barton, J. K. *J. Am. Chem. Soc.* **1997**, 119, 9861–9870.
- (8) Kelley, S. O.; Barton, J. K.; Jackson, N. M.; McPherson, L. D.; Potter, A. B.; Spain, E. M.; Allen, M. J.; Hill, M. G. *Langmuir* **1998**, 14, 6781–6784.
- (9) Kelley, S. O.; Barton, J. K. *Science* **1999**, 283, 375–381.
- (10) Nunez, M. E.; Hall, D. B.; Barton, J. K. *Chem. Biol.* **1999**, 6, 85–97.
- (11) Wan, C. Z.; Fiebig, T.; Kelley, S. O.; Treadway, C. R.; Barton, J. K.; Zewail, A. H. *Proc. Natl. Acad. Sci. U.S.A.* **1999**, 96, 6014–6019.
- (12) Wan, C. Z.; Fiebig, T.; Schiemann, O.; Barton, J. K.; Zewail, A. H. *Proc. Natl. Acad. Sci. U.S.A.* **2000**, 97, 14052–14055.
- (13) Williams, T. T.; Odom, D. T.; Barton, J. K. *J. Am. Chem. Soc.* **2000**, 122, 9048–9049.
- (14) (a) Fukui, K.; Tanaka, K. *Angew. Chem., Int. Ed. Engl.* **1998**, 37, 158–161. (b) Hess, S.; Gotz, M.; Davis, W. B.; Michel-Beyerle, M. E. *J. Am. Chem. Soc.* **2001**, 123, 10046–10055.
- (15) Fukui, K.; Tanaka, K.; Fujitsuka, M.; Watanabe, A.; Ito, O. *J. Photochem. Photobiol., B* **1999**, 50, 18–27.
- (16) Fukui, K. *Electrochem.* **2000**, 68, 992–995.
- (17) Meggers, E.; Kusch, D.; Spichty, M.; Wille, U.; Giese, B. *Angew. Chem., Int. Ed. Engl.* **1998**, 37, 460–462.
- (18) Meggers, E.; Michel-Beyerle, M. E.; Giese, B. *J. Am. Chem. Soc.* **1998**, 120, 12950–12955.
- (19) Giese, B.; Wessely, S.; Spormann, M.; Lindemann, U.; Meggers, E.; Michel-Beyerle, M. E. *Angew. Chem., Int. Ed. Engl.* **1999**, 38, 996–998.
- (20) Davis, W. B.; Naydenova, I.; Haselsberger, R.; Ogrodnik, A.; Giese, B.; Michel-Beyerle, M. E. *Angew. Chem., Int. Ed. Engl.* **2000**, 39, 3649–3652.
- (21) Giese, B.; Spichty, M. *Chem. Phys. Chem.* **2000**, 1, 195–198.
- (22) Giese, B.; Wessely, S. *Angew. Chem., Int. Ed. Engl.* **2000**, 39, 3490.
- (23) Giese, B. *Acc. Chem. Res.* **2000**, 33, 631–636.
- (24) Brun, A. M.; Harriman, A. *J. Am. Chem. Soc.* **1992**, 114, 3656–3660.
- (25) Brun, A. M.; Harriman, A. *J. Am. Chem. Soc.* **1994**, 116, 10383–10393.
- (26) Harriman, A. *Angew. Chem., Int. Ed. Engl.* **1999**, 38, 945–949.
- (27) Lewis, F. D.; Wu, T. F.; Zhang, Y. F.; Letsinger, R. L.; Greenfield, S. R.; Wasielewski, M. R. *Science* **1997**, 277, 673–676.
- (28) Lewis, F. D.; Letsinger, R. L. *J. Phys. Chem.* **1998**, 3, 215–221.
- (29) Lewis, F. D.; Liu, X. Y.; Miller, S. E.; Wasielewski, M. R. *J. Am. Chem. Soc.* **1999**, 121, 9746–9747.
- (30) Lewis, F. D.; Liu, X. Y.; Wu, Y. S.; Miller, S. E.; Wasielewski, M. R.; Letsinger, R. L.; Sanishvili, R.; Joachimiak, A.; Tereshko, V.; Egli, M. *J. Am. Chem. Soc.* **1999**, 121, 9905–9906.
- (31) Lewis, F. D.; Wu, T. F.; Liu, X. Y.; Letsinger, R. L.; Greenfield, S. R.; Miller, S. E.; Wasielewski, M. R. *J. Am. Chem. Soc.* **2000**, 122, 2889–2902.
- (32) Lewis, F. D.; Liu, X. Y.; Liu, J. Q.; Miller, S. E.; Hayes, R. T.; Wasielewski, M. R. *Nature* **2000**, 406, 51–53.
- (33) Lewis, F. D.; Liu, X. Y.; Liu, J. Q.; Hayes, R. T.; Wasielewski, M. R. *J. Am. Chem. Soc.* **2000**, 122, 12037–12038.
- (34) Lewis, F. D.; Kalgutkar, R. S.; Wu, Y.; Liu, X.; Liu, J.; Hayes, R. T.; Miller, S. H.; Wasielewski, M. R. *J. Am. Chem. Soc.* **2000**, 122, 12346–12351.
- (35) (a) Lewis, F. D.; Letsinger, R. L.; Wasielewski, M. R. *Acc. Chem. Res.* **2000**. (b) Lewis, F. D.; Liu, J.; Weigel, W.; Rettig, W.; Kurnikov, I. V.; Beratan, D. N. **2002**, in preparation.
- (36) Meade, T. J.; Kayyem, J. F. *Angew. Chem., Int. Ed. Engl.* **1995**, 34, 352–354.



- (37) Breslin, D. T.; Schuster, G. B. *J. Am. Chem. Soc.* **1996**, *118*, 2311–2319.
- (38) Ly, D.; Kan, Y. Z.; Armitage, B.; Schuster, G. B. *J. Am. Chem. Soc.* **1996**, *118*, 8747–8748.
- (39) Gasper, S. M.; Schuster, G. B. *J. Am. Chem. Soc.* **1997**, *119*, 12762–12771.
- (40) Henderson, P. T.; Jones, D.; Hampikian, G.; Kan, Y. Z.; Schuster, G. B. *Proc. Natl. Acad. Sci. U.S.A.* **1999**, *96*, 8353–8358.
- (41) Ly, D.; Sani, L.; Schuster, G. B. *J. Am. Chem. Soc.* **1999**, *121*, 9400–9410.
- (42) Schuster, G. B. *Acc. Chem. Res.* **2000**, *33*, 253–260.
- (43) Sani, L.; Schuster, G. B. *J. Am. Chem. Soc.* **2000**, *122*, 11545–11546.
- (44) Risser, S. M.; Beratan, D. N.; Meade, T. J. *J. Am. Chem. Soc.* **1993**, *115*, 2508–2510.
- (45) Priyadarshy, S.; Beratan, D. N.; Risser, S. M. *Int. J. Quantum Chem.* **1996**, *60*, 65–71.
- (46) Priyadarshy, S.; Risser, S. M.; Beratan, D. N. *J. Phys. Chem.* **1996**, *100*, 17678–17682.
- (47) Beratan, D. N.; Priyadarshy, S.; Risser, S. M. *Chem. Biol.* **1997**, *4*, 3–8.
- (48) Priyadarshy, S.; Risser, S. M.; Beratan, D. N. *JBIC* **1998**, *3*, 196–200.
- (49) Ratner, M. *Nature* **1999**, *397*, 480–481.
- (50) Grozema, F. C.; Berlin, Y. A.; Siebbeles, L. D. A. *Int. J. Quantum Chem.* **1999**, *75*, 1009–1016.
- (51) Berlin, Y. A.; Burin, A. L.; Ratner, M. A. *J. Phys. Chem. A* **2000**, *104*, 443–445.
- (52) Berlin, Y. A.; Burin, A. L.; Ratner, M. A. *Superlat. Microstruct.* **2000**, *28*, 241–252.
- (53) Grozema, F. C.; Berlin, Y. A.; Siebbeles, L. D. A. *J. Am. Chem. Soc.* **2000**, *122*, 10903–10909.
- (54) Berlin, Y. A.; Burin, A. L.; Ratner, M. *J. Am. Chem. Soc.* **2001**, *123*, 260–268.
- (55) Berlin, Y. A.; Burin, A. L.; Siebbeles, L. D. A.; Ratner, M. A. *J. Phys. Chem. A* **2001**, *105*, 5666–5678.
- (56) Bixon, M.; Jortner, J. *J. Phys. Chem. B* **2000**, *104*, 3906–3913.
- (57) Jortner, J.; Bixon, M.; Langenbacher, T.; Michel-Beyerle, M. E. *Proc. Natl. Acad. Sci. U.S.A.* **1998**, *95*, 12759–12765.
- (58) Jortner, J.; Bixon, M.; Langenbacher, T.; Michel-Beyerle, M. E. *Biophys. J.* **1999**, *76*, A263.
- (59) Bixon, M.; Giese, B.; Wessely, S.; Langenbacher, T.; Michel-Beyerle, M. E.; Jortner, J. *Proc. Natl. Acad. Sci. U.S.A.* **1999**, *96*, 11713–11716.
- (60) Voityuk, A. A.; Jortner, J.; Bixon, M.; Rosch, N. *Chem. Phys. Lett.* **2000**, *324*, 430–434.
- (61) Voityuk, A. A.; Rosch, N.; Bixon, M.; Jortner, J. *J. Phys. Chem. B* **2000**, *104*, 9740–9745.
- (62) Voityuk, A. A.; Jortner, J.; Bixon, M.; Rosch, N. *J. Chem. Phys.* **2001**, *114*, 5614–5620.
- (63) Conwell, E. M.; Rakhmanova, S. V. *Proc. Natl. Acad. Sci. U.S.A.* **2000**, *97*, 4556–4560.
- (64) Rakhmanova, S. V.; Conwell, E. M. *J. Phys. Chem. B* **2001**, *105*, 2056–2061.
- (65) Felts, A. K.; Pollard, W. T.; Friesner, R. A. *J. Phys. Chem.* **1995**, *99*, 2929–2940.
- (66) Okada, A.; Chernyak, V.; Mukamel, S. *J. Phys. Chem. A* **1998**, *102*, 1241–1251.
- (67) Yan, Y. J.; Li, X. Q.; Zhang, H. Y. *J. Chem. Phys.* **2001**, *114*, 8248–8250.
- (68) Burrows, C. J.; Muller, J. G. *Chem. Rev.* **1998**, *98*, 1109–1151.
- (69) Armitage, B. *Chem. Rev.* **1998**, *98*, 1171–1200.
- (70) Heelis, P. F.; Hartman, R. F.; Rose, S. D. *Chem. Soc. Rev.* **1995**, *24*, 289–&.
- (71) Park, H. W.; Kim, S. T.; Sancar, A.; Deisenhofer, J. *Science* **1995**, *268*, 1866–1872.
- (72) Thorp, H. H. *Trends Biotechnol.* **1998**, *16*, 117–121.
- (73) Kelley, S. O.; Jackson, N. M.; Hill, M. G.; Barton, J. K. *Angew. Chem., Int. Ed. Engl.* **1999**, *38*, 941–945.
- (74) Wang, J.; Bollo, S.; Paz, J. L. L.; Sahlin, E.; Mukherjee, B. *Anal. Chem.* **1999**, *71*, 1910–1913.
- (75) Armistead, P. M.; Thorp, H. H. *Anal. Chem.* **2000**, *72*, 3764–3770.
- (76) Alivisatos, A. P.; Johnsson, K. P.; Peng, X. G.; Wilson, T. E.; Loweth, C. J.; Bruchez, M. P.; Schultz, P. G. *Nature* **1996**, *382*, 609–611.
- (77) Ratner, M. A.; Jortner, J. *Molecular Electronics*; Blackwell Science: Oxford, 1997.
- (78) Braun, E.; Eichen, Y.; Sivan, U.; Ben Yoseph, G. *Nature* **1998**, *391*, 775–778.
- (79) Okahata, Y.; Kobayashi, T.; Tanaka, K.; Shimomura, M. *J. Am. Chem. Soc.* **1998**, *120*, 6165–6166.
- (80) Okahata, Y.; Niikura, K.; Furusawa, H.; Matsuno, H. *Anal. Sci.* **2000**, *16*, 1113–1119.
- (81) Winfree, E.; Liu, F. R.; Wenzler, L. A.; Seeman, N. C. *Nature* **1998**, *394*, 539–544.
- (82) Fink, H. W.; Schonenberger, C. *Nature* **1999**, *398*, 407–410.
- (83) Storhoff, J. J.; Mirkin, C. A. *Chem. Rev.* **1999**, *99*, 1849–1862.
- (84) Mirkin, C. A.; Taton, T. A. *Nature* **2000**, *405*, 626–627.
- (85) Porath, D.; Bezryadin, A.; de Vries, S.; Dekker, C. *Nature* **2000**, *403*, 635–638.
- (86) Bixon, M.; Jortner, J. *Adv. Chem. Phys.* **1999**, *106*, 35–202.
- (87) Davis, W. B.; Wasielewski, M. R.; Ratner, M. A.; Mujica, V.; Nitzan, A. *J. Phys. Chem. A* **1997**, *101*, 6158–6164.
- (88) Marcus, R. A.; Sutin, N. *Biochim. Biophys. Acta* **1985**, *811*, 265–322.
- (89) Wasielewski, M. R. *Chem. Rev.* **1992**, *92*, 435–461.
- (90) Paulson, B.; Pramod, K.; Eaton, P.; Closs, G.; Miller, J. R. *J. Phys. Chem.* **1993**, *97*, 13042–13045.
- (91) Winkler, J. R.; Gray, H. B. *Chem. Rev.* **1992**, *92*, 369–379.
- (92) Kuznetsov, A. M.; Ulstrup, J. *Phys. Stat. Solidi B* **1982**, *114*, 673–683.
- (93) (a) Hopfield, J. J. *Proc. Natl. Acad. Sci. U.S.A.* **1974**, *71*, 3640–3644. (b) J. N. Onuchic, J. N.; Beratan, D. N.; Hopfield, J. J. *J. Phys. Chem.* **1986**, *90*, 3707–3721.
- (94) Newton, M. D. *Chem. Rev.* **1991**, *91*, 767–792.
- (95) Daizadeh, I.; Gehlen, J. N.; Stuchebrukhov, A. A. *J. Chem. Phys.* **1997**, *106*, 5658–5666.
- (96) Katz, D. J.; Stuchebrukhov, A. A. *J. Chem. Phys.* **1998**, *109*, 4960–4970.
- (97) Ivashin, N.; Kallebring, B.; Larsson, S.; Hansson, O. *J. Phys. Chem. B* **1998**, *102*, 5017–5022.
- (98) Priyadarshy, S.; Skourtis, S. S.; Risser, S. M.; Beratan, D. N. *J. Chem. Phys.* **1996**, *104*, 9473–9481.
- (99) Kurnikov, I. V.; Zusman, L. D.; Kurnikova, M. G.; Farid, R. S.; Beratan, D. N. *J. Am. Chem. Soc.* **1997**, *119*, 5690–5700.
- (100) Kumar, K.; Kurnikov, I. V.; Beratan, D. N.; Waldeck, D. H.; Zimmt, M. B. *J. Phys. Chem. A* **1998**, *102*, 5529–5541.
- (101) Sharp, K. A. *Biophys. J.* **1998**, *74*, 1241–1250.
- (102) Tavernier, H. L.; Fayer, M. D. *J. Phys. Chem. B* **2000**, *104*, 11541–11550.
- (103) Meggers, E.; Giese, B. *Nucleosides Nucleotides* **1999**, *18*, 1317–1318.
- (104) Kelley, S. O.; Barton, J. K. *Chem. Biol.* **1998**, *5*, 413–425.
- (105) Balabin, I. A.; Onuchic, J. N. *J. Phys. Chem. B* **1998**, *102*, 7497–7505.
- (106) Balabin, I. A.; Onuchic, J. N. *Science* **2000**, *290*, 114–117.
- (107) Marcus, R. A.; Sutin, N. *Biochim. Biophys. Acta* **1985**, *811*, 265–322.
- (108) Beratan, D. N.; Onuchic, J. N.; Winkler, J. R.; Gray, H. B. *Science* **1992**, *258*, 1740–1741.
- (109) Gray, H. B.; Winkler, J. R. *Annu. Rev. Biochem.* **1996**, *65*, 537–561.
- (110) Winkler, J. R.; Gray, H. B. *JBIC* **1997**, *2*, 399–404.
- (111) Winkler, J. R. *Curr. Opin. Chem. Biol.* **2000**, *4*, 192–198.
- (112) Barber, J.; Andersson, B. *Nature* **1994**, *370*, 31–34.
- (113) Sivaraja, M.; Goodin, D. B.; Smith, M.; Hoffman, B. M. *Science* **1989**, *245*, 738–740.
- (114) Houseman, A. L. P.; Doan, P. E.; Goodin, D. B.; Hoffman, B. M. *Biochem.* **1993**, *32*, 4430–4443.
- (115) Huyett, J. E.; Doan, P. E.; Gurbel, R.; Houseman, A. L. P.; Sivaraja, M.; Goodin, D. B.; Hoffman, B. M. *J. Am. Chem. Soc.* **1995**, *117*, 9033–9041.
- (116) RodriguezMonge, L.; Larsson, S. *J. Phys. Chem.* **1996**, *100*, 6298–6303.
- (117) Jordan, K. D.; Paddonrow, M. N. *J. Phys. Chem.* **1992**, *96*, 1188–1196.
- (118) Liang, C. X.; Newton, M. D. *J. Phys. Chem.* **1992**, *96*, 2855–2866.
- (119) Kurnikov, I. V.; Beratan, D. N. *J. Chem. Phys.* **1996**, *105*, 9561–9573.
- (120) Larsson, S. *J. Chem. Soc., Faraday Trans. 2* **1983**, *79*, 1375–1388.
- (121) Sitkoff, D.; Sharp, K. A.; Honig, B. *J. Phys. Chem.* **1994**, *98*, 1978–1988.
- (122) Liu, Y. P.; Newton, M. D. *J. Phys. Chem.* **1995**, *99*, 12382–12386.
- (123) Wolfgang, J.; Risser, S. M.; Priyadarshy, S.; Beratan, D. N. *J. Phys. Chem. B* **1997**, *101*, 2986–2991.
- (124) Lewis, F. D. Private communications.
- (125) Dolgounitcheva O.; Zakrzewski V. G.; Ortiz J. V. *Int. J. Quantum Chem.* **2000**, *80*, 831–835.